HHS Public Access

Author manuscript

Birth Defects Res. Author manuscript; available in PMC 2020 January 02.

Published in final edited form as:

Birth Defects Res. 2019 November 15; 111(19): 1520–1534. doi:10.1002/bdr2.1591.

Deletion of neural tube defect-associated gene *Mthfd1l* causes reduced cranial mesenchyme density

Minhye Shin, **Amanda Vaughn**, **Jessica Momb**, **Dean R. Appling**

Department of Molecular Biosciences, The University of Texas at Austin, Austin, Texas

Abstract

Background: Periconceptional intake of supplemental folic acid can reduce the incidence of neural tube defects by as much as 70%, but the mechanisms by which folic acid supports cellular processes during neural tube closure are unknown. The mitochondrial 10-formyl-tetrahydrofolate synthetase MTHFD1L catalyzes production of formate, thus generating one-carbon units for cytoplasmic processes. Deletion of *Mthfd1l* causes embryonic lethality, developmental delay, and neural tube defects in mice.

Methods: To investigate the role of mitochondrial one-carbon metabolism during cranial neural tube closure, we have analyzed cellular morphology and function in neural tissues in *Mthfd1l* knockout embryos.

Results: The head mesenchyme showed significantly lower cellular density in *Mthfd1l* nullizygous embryos compared to wildtype embryos during the process of neural tube closure. Apoptosis and neural crest cell specification were not affected by deletion of *Mthfd1l*. Sections from the cranial region of *Mthfd1l* knockout embryos exhibited decreased cellular proliferation, but only after completion of neural tube closure. Supplementation of pregnant dams with formate improved mesenchymal density and corrected cell proliferation in the nullizygous embryos.

Conclusions: Deletion of *Mthfd1l* causes decreased density in the cranial mesenchyme and this defect is improved with formate supplementation. This study reveals a mechanistic link between folate-dependent mitochondrially produced formate, head mesenchyme formation and neural tube defects.

Keywords

folate; head mesenchyme; MTHFD1L; neural tube closure; neural tube defects; proliferation

1 | INTRODUCTION

Closure of the neural tube during development is a highly complex but poorly understood process (Juriloff & Harris, 2018; Nikolopoulou, Galea, Rolo, Greene, & Copp, 2017). Neural tube defects (NTDs) have a multifactorial etiology, including both genetic and environmental factors. The importance of maternal folate status to NTD risk was first

Correspondence Dean R. Appling, Department of Molecular Biosciences, The University of Texas at Austin, Austin, TX 78712. dappling@austin.utexas.edu.

suggested more than 40 years ago (Hibbard & Smithells,1965). Periconceptional intake of supplemental folic acid can reduce the incidence of NTDs by as much as 70%, and many countries now fortify their food supply with folic acid to ensure that women of child-bearing age consume adequate quantities of the vitamin. While folic acid fortification has decreased NTD incidence in most populations, an estimated 30% of NTD cases do not respond to folic acid supplementation (Hobbs, Shaw, Werler, & Mosley, 2010). Moreover, despite the strong clinical links between folate and NTDs, the biochemical mechanisms through which folic acid acts during neural tube development remain largely undefined (Au, Findley, & Northrup, 2017).

One-carbon (1C) metabolism is a universal folate-dependent pathway that generates 1C units for de novo purine and thymidylate synthesis, interconversion of several amino acids, production of universal methyl donors, and regeneration of redox cofactors. One-carbon metabolism is highly compartmentalized in eukaryotes (Tibbetts & Appling, 2010), and mitochondria play a critical role in cellular 1C metabolism (Figure 1). Mitochondria import 1C donors such as serine and glycine and oxidize the 1C units to formate, which is exported to the cytoplasm as a 1C unit for synthesis of purines, thymidylate, and methyl groups (Momb et al., 2013; Pike, Rajendra, Artzt, & Appling, 2010). These cytosolic and mitochondrial pathways are metabolically connected, supporting a mostly unidirectional flow of 1C units (clockwise in Figure 1). Interconversion of 1C units in mammalian mitochondria is catalyzed by three distinct members of the MTHFD (methylenetetrahydrofolate dehydrogenase) family of enzymes: MTHFD2L, MTHFD2, and MTHFD1L (Figure 1). MTHFD1L is a 10-formyl-tetrahydrofolate (10-CHO-THF) synthetase, catalyzing the final step in the mitochondrial pathway to produce formate, thus controlling the flux of 1C units from mitochondria into cytoplasmic processes (Bryant et al., 2018). The *Mthfd1l* gene is expressed ubiquitously throughout the mouse embryo at all stages of embryogenesis with localized regions of higher expression along the neural tube, the brain, craniofacial structures, limb buds, and the tail bud in E9.5–13.5 whole embryos (Momb et al., 2013; Pike et al., 2010; Shin, Bryant, Momb, & Appling, 2014).

Mouse embryos lacking MTHFD1L exhibit aberrant neural tube closure, craniofacial defects, developmental delay, and embryonic lethality by embryonic day 12.5 (E12.5) (Momb et al., 2013). Homozygous deletion of *Mthfd1l* results in NTDs with 100% penetrance, even on a folate-replete diet. The NTD phenotype is variable, including defects such as wavy neural tube, exencephaly, and craniorachischisis. Spina bifida is not observed in this mouse model. Consistent with the prediction that lack of 10-CHO-THF synthetase activity would result in a loss of mitochondrial formate production, supplementation of pregnant dams with formate reduces the incidence of neural tube defects, partially rescues growth restriction, and significantly extends survival of null embryos (Momb et al., 2013).

Despite the clear association of MTHFD1L and folate-mediated 1C metabolism with NTDs, the cellular mechanisms by which folate, mitochondrially derived formate, and 1C metabolism support normal neural tube closure are not understood. Because exencephaly is the most commonly occurring NTD in the *Mthfd1l* KO mouse model, we chose to focus on the cranial region in this study. To investigate the role of 1C metabolism during cranial neural tube closure, several cellular processes were analyzed in *Mthfd1l* knockout mice

during neural tube closure, including head mesenchyme formation, cell proliferation, apoptosis, and neural crest cell specification. These same processes were investigated in *Mthfd1l*-null embryos supplemented with formate to understand how mitochondrially produced formate facilitates cranial neural tube closure. In this study, we show that deletion of *Mthfd1l* causes reduced cranial mesenchyme density that can be corrected with maternal formate supplementation. Our results reveal no differences in apoptosis or neural crest cell specification in the developing cranial region of *Mthfd1l* KO embryos, but cell proliferation is reduced, and formate supplementation improves the observed phenotype. Importantly, we observe that cellular density in the cranial mesenchyme of *Mthfd1l* KO embryos is severely reduced compared to WT embryos, and this defect is improved with formate supplementation, suggesting that mitochondrial formate production is critical for head mesenchyme formation.

2 | METHODS

2.1 | Mice

All protocols used in this study were approved by the Institutional Animal Care and Use Committee of The University of Texas at Austin and performed within the guidelines of the National Institutes of Health for the Care and Use of Laboratory Animals. *Mthfd1l* (methylenetetrahydrofolate dehydrogenase ($NADP^+$-dependent) 1-like) heterozygous mice were maintained on a C57BL/6 genetic background and genotyped as described previously (Momb et al., 2013). All mice were fed standard commercially available laboratory chow (LabDiet 5K67) and exposed to a 12 hr light–dark cycle.

2.2 | Embryo isolation and preparation

Embryos of three different genotypes were generated by mating $Mthfd1l^{z/+}$ heterozygous males and females. Appearance of a vaginal plug was designated as embryonic day (E) 0.5, and embryos were dissected within specific somite number ranges: 7–13 somites (approximately E8.5–E8.75 for $Mthfd1l^{+/+}$ wild types and E9.5 for $Mthfd1l^{z/z}$ nullizygotes); and 18–24 somites (approximately E9.5 for wild types and E10.5 for nullizygotes). These somite ranges were chosen to represent the characteristic morphology of the neural tube closure and are roughly comparable to Theiler Stages (TS) TS13 (8–12 somites) and TS15 (21–29 somites) (Theiler, 1989). Gross morphology and neural tube closure were examined. Neural tube closure in the cranial region was scored as open if any part of the neural tube was not closed. For immunohistochemistry, embryos were fixed for 30 min (E8.5), 1.5 hr (E9.5), or 3 hr (E10.5) at 4 °C in 4% (wt/vol) paraformaldehyde in PBS, pH 7.2, washed twice in PBS and infused in 30% (wt/vol) sucrose in PBS overnight and frozen. For whole mount in situ hybridization (ISH) assay, embryos were fixed overnight at 4 C in 4% (wt/vol) paraformaldehyde in PBS, pH 7.2, washed twice in PBS and dehydrated and stored in 100% methanol at −20 °C before processing for in situ hybridization. For hematoxylin and eosin (H&E) staining, embryos were fixed overnight at 4 C in 4% (wt/vol) paraformaldehyde in PBS, pH 7.2, washed twice in PBS, dehydrated with ethanol, and embedded in paraffin. Paraffin-embedded embryo sections were stained with H&E (American Mastertech Scientific, Inc.)

2.3 | Immunohistochemistry

Embryos were cryosectioned in optimal cutting temperature medium. Cryosections (7 μm) were blocked in 0.5% (vol/vol) Triton in PBS (PBST) containing 5% normal goat serum for 30 min at room temperature. For cleaved caspase-3, 2% (wt/vol) BSA was added to the blocking solution and the sections were blocked for 1.5 hr. Primary antibodies were applied overnight at 4 °C: anti-phosphohistone H3 (Millipore #06–570; 1:300 dilution), and anti-cleaved caspase 3 (Cell Signaling #9664; 1:200 dilution). Secondary antibodies were goat anti-rabbit IgG Alexa Fluor 555 (Cell Signaling #4413; 1:200 dilution) and goat anti-mouse IgG Alexa Fluor 488 (Life Technologies #A11017; 1:200 dilution). At least three embryos were assessed with each anti-body. For nuclear staining, cells were incubated with anti-fade mounting medium with DAPI (Vectashield #H1200). Fluorescent images were collected by a 20× objective lens using an Axiovert 200M fluorescence microscope (Zeiss). Four layers were stitched together using Zeiss AxioVision software (release 4.8.2) to create composite section images which were analyzed using ImageJ software (U.S. National Institutes of Health). To calculate the mitotic index or the apoptotic index, the number of cells exhibiting a positive immunostaining signal for phosphohistone H3 (PHH3) or cleaved caspase-3, respectively, was divided by total cell number of neuroepithelium or mesenchyme in the embryo section (for the mitotic index) or by total cell number in the whole embryo section (for the apoptotic index).

2.4 | Whole mount in situ hybridization

Mouse embryos ranging from E8.5 to E10.5 were hybridized using digoxigenin-labeled RNA probes (Wilkinson, 1998). The plasmid harboring *Sox9* was a gift from Dr. Steven Vokes and a plasmid harboring *FoxD3* was purchased from Addgene (Cambridge, MA; plasmid #37098).

2.5 | Quantitative analysis of head mesenchyme cell density

Quantitative analysis of head mesenchyme cell density was carried out based on a previously described method (Dunlevy, Burren, Mills, et al., 2006). Cryosections of embryos were stained with DAPI and paraffin-embedded sections were stained with H&E. Cell counting areas were defined as a percentage of the section being investigated by using boxes of defined dimensions located in a central site (8.5% × 33.5% of each section width) or a lateral site (8.5% × 16.7% of each section width). Image processing was conducted using ImageJ.

2.6 | Histology

For histological analysis, fixed embryos were washed twice with room temperature PBS, dehydrated in an ethanol gradient and transferred into Xylene Substitute (Histo-Clear, National Diagnostics) twice for 5 min. Embryos were then embedded in paraffin and sectioned at 7 μm and mounted on negatively charged glass microscope slides. Sections were stained with H&E (American Mastertech Scientific, Inc.) and imaged using a Nikon Eclipse Compound Microscope.

2.7 | Ethynyl-deoxyuridine (EdU) incorporation in mouse embryonic fibroblasts

Mouse embryonic fibroblasts (MEFs), derived from pools of wild-type and *Mthfd1l*$^{gt/gt}$ embryos respectively, were plated at a density of 5,000 cells per well and cultured for 24 hr in basal medium (DMEM), minimal medium (MEM), or minimal medium with 1 mM sodium formate supplementation (MEM+F). After addition of 10 μM EdU in PBS (Invitrogen), cells were incubated for 2 hr, fixed and processed for detection of EdU (Click-It EdU Imaging Kit). For simultaneous detection of mitosis, cells were washed in PBST buffer containing 0.5% Triton-X100 and blocked for 30 min in PBST containing 5% normal goat serum, 0.15% (wt/vol) glycine, and 2 mg/ml BSA prior to immunohisto-chemistry for phosphohistone H3.

2.8 | Maternal supplementation with calcium formate

Formate supplementation was achieved by the addition of calcium formate to the drinking water of *Mthfd1l*$^{gt/+}$ mating pairs. Concentration of calcium formate was 0.1 M to deliver 2,500 mg formate kg^{-1} d^{-1}, based on an average water intake of 5 ml per day for a 25 g C57BL/6 mouse (Momb et al., 2013). The effect of formate supplementation on somite numbers/crown-rump length, head mesenchyme density and proliferation were analyzed.

2.9 | Statistical analysis

All quantitative data were compared using one- or two-way analysis of variance, or Mann–Whitney *U* test. All statistical tests were performed using Prism version 7 (GraphPad, La Jolla, CA).

3 | RESULTS

3.1 | Deletion of *Mthfd1l* impairs embryonic growth and development

Our initial report on the effect of *Mthfd1l* deletion on embryonic growth and development analyzed the morphology of embryos at E10.5 or later, after neural tube closure is complete (Momb et al., 2013). Since neural tube closure begins around E8.5 in mouse embryos (Yamaguchi & Miura, 2013), here we collected litters at a series of developmental stages from E8.5 to E10.5. The number of embryos of each genotype conformed to expected Mendelian inheritance ratios at earlier stages of development (E8.5–9.5) but not at the later stage (E10.5) (Table 1). This result is consistent with our previous report that deletion of *Mthfd1l* is embryonic lethal and *Mthfd1l*$^{gt/gt}$ (nullizygote) embryos die by E12.5 (Momb et al., 2013). As embryo age increased from E8.5 to 10.5, the percentage of embryos with closed cranial neural tubes increased for all genotypes, however a significant number of *Mthfd1l*$^{gt/gt}$ embryos retained an open cranial neural tube at E10.5 (Table 1). The *Mthfd1l*$^{gt/gt}$ embryos whose neural tubes had closed in the cranial region were small and pale with a wavy neural tube and abnormally shaped head, consistent with the phenotype we previously observed in *Mthfd1l*$^{gt/gt}$ embryos at E11.5 and E12.5 (Momb et al., 2013). Open neural tubes were observed in a few wild-type and *Mthfd1l*$^{gt/+}$ embryos at E9.5 and E10.5 (Table 1), which is after the point that the neural tube is typically closed in wild-type mouse strains. This may indicate a phenotype due to the maternal *Mthfd1l*$^{gt/+}$ genotype and/or an interaction between the embryo and maternal genotypes.

The growth and development of *Mthfd1l*$^{gt/tz}$ embryos was severely retarded compared to *Mthfd1l*$^{gt/+}$ and *Mthfd1l*$^{+/+}$ embryos, with *Mthfd1l*$^{gt/tz}$ embryos exhibiting significantly fewer somites at all observed gestational timepoints (E8.5 to E10.5, $p < .001$), equivalent to a developmental delay of approximately 0.75 day (Table 1). Correspondingly, the mean crown-rump length of *Mthfd1l*-deficient embryos was also smaller at E8.5, E9.5, and E10.5 (Table 1). A plot of crown to rump length versus somite number for individual embryos shows no significant difference between genotypes until the number of somites exceeds 35 (Figure 2).

3.2 | Deletion of *Mthfd1l* causes a defect in head mesenchyme development during early neural tube closure

The head mesenchyme in *Mthfd1l*$^{gt/tz}$ embryos appeared sparser in the hindbrain, especially underneath the neural plate. To examine the cell density of head mesenchyme, transverse cryosections of 7–13 somite stage *Mthfd1l*$^{+/+}$ and *Mthfd1l*$^{gt/tz}$ embryos were stained with DAPI to visualize nuclei, and cell density in the head mesenchyme was quantified (Figure 3a,b). The total mesenchyme density was significantly lower in the mutant embryos compared to wild-type embryos (Figure 3e). The decrease in cell density was most apparent in the mesenchyme underlying the neural plate (central boxed area, Figure 3a–c). The apparent difference around the lateral edges of neural plate (lateral boxed areas, Figure 3a,b,d) did not reach statistical significance. To address a possible confounding effect of developmental difference between the two genotypes, we segregated the embryos into subgroups covering a narrower range of somite stages (7–9 and 10–13 somite stages, respectively). The central and total head mesenchyme density was significantly lower in *Mthfd1l*$^{gt/tz}$ embryos for both the 7–9 and 10–13 subgroups (Figure 3c,e). Moreover, Figure 3f shows that the wild-type and *Mthfd1l*-null embryos examined in this experiment were distributed similarly across the 7–13 somite range. These data suggest that development of the head mesenchyme is abnormal in *Mthfd1l*$^{gt/tz}$ embryos.

To examine the mesenchyme defect using a method with better morphological preservation, cranial tissue from embryos at the 7–13 somite stage was paraffin-processed, sectioned, and stained with stained with H&E (Figure 4a,b). This method also showed a trend toward reduced mesenchyme density in *Mthfd1l*$^{gt/tz}$ embryos, but did not reach statistical significance (Figure 4c).

Formate supplementation of the dams improved the development of head mesenchyme in null embryos at the 7–13 somite stage (Figure 5a,b). Head mesenchyme cell density was normalized in central and lateral areas, as well as in total sections (Figure 5c–e). These results indicate that mitochondrially derived formate provided by MTHFD1L activity is essential for the development of cranial mesenchyme.

3.3 | Deletion of *Mthfd1l* decreases cellular proliferation in hindbrain neuroepithelium at timepoints after completion of neural tube closure

The mitotic index was compared in the neuroepithelium of *Mthfd1l*$^{+/+}$ (wild-type) and *Mthfd1l*$^{gt/tz}$ (nullizygous) embryos at the 7–13 somite stage during initiation of neural tube closure and at the 18–24 somite stage after completion of neural tube closure. Representative

sections of phosphohistone H3 (PHH3) immunofluorescence staining show the characteristic apical location of mitotic nuclei in the neuroepithelium of *Mthfd1l*$^{+/+}$ and *Mthfd1l*$^{gt/gt}$ embryos (Figure 6). The mitotic index of the hindbrain region of *Mthfd1l*$^{gt/gt}$ embryos is significantly decreased at the 18–24 somite stage after completion of neural tube closure (Figure 6f, $p = .016$), but not at the 7–13 somite stage when neural tube closure is being initiated (Figure 6e, $p = .69$).

To determine if the decreased density of the head mesenchyme in *Mthfd1l*$^{gt/gt}$ embryos results from a change in proliferation, expression of phosphohistone H3 (PHH3) was examined in the mesenchyme at the 7–13 somite stage. The mitotic index in the head mesenchyme of *Mthfd1l*$^{gt/gt}$ embryos was not significantly different compared with *Mthfd1l*$^{+/+}$ embryos (Figure 6g), indicating no difference in proliferation of the abnormal head mesenchyme surrounding the neural tube.

To investigate whether decreased proliferation is observed in isolated cultured *Mthfd1l*$^{gt/gt}$ cells, ethynyl-deoxyuridine (EdU) incorporation and PHH3 expression were determined in primary mouse embryonic fibroblast (MEF) cultured cells. MEFs were grown in basal medium (DMEM), minimal medium (MEM), or minimal medium with formate supplementation (MEM+F). Although *Mthfd1l*$^{gt/gt}$ MEFs grew slowly in the minimal medium, the EdU incorporation and PHH3 expression did not differ significantly between *Mthfd1l*$^{+/+}$ and *Mthfd1l*$^{gt/gt}$ MEFs in any of the growth conditions investigated (Table 2).

3.4 | Formate supplementation improves embryonic growth development and cellular processes

As previously reported (Momb et al., 2013), maternal supplementation with formate partially rescued growth defects in *Mthfd1l*$^{gt/gt}$ embryos. At E8.75, the genotype distribution did not differ significantly from the expected Mendelian ratio (Table 3, $p = .85$; cf. Table 1).

Formate supplementation also reduced the differences observed between wild-type and null embryos in somite number and crown-to-rump length (Table 3; cf. Table 1). Importantly, formate supplementation corrected the defect in hindbrain neuroepithelium proliferation that was observed in unsupplemented *Mthfd1l*$^{gt/gt}$ embryos at the 18–24 somite stage (Figure 7, $p = .70$).

3.5 | Deletion of *Mthfd1l* has no effect on apoptosis in cranial tissue

Caspase-3 staining was used to examine the distribution of apoptotic cells in the cranial regions of *Mthfd1l*$^{+/+}$ and *Mthfd1l*$^{gt/gt}$ embryos. Cleaved caspase-3 staining of embryos of both genotypes revealed the presence of apoptotic cells at the sites of dorsolateral bending of the neural plate, and at the tips of the fusing neural folds (Figure 8). The number of apoptotic cells increased at the 18–24 somite stages by 6.0- and 3.8-fold in *Mthfd1l*$^{+/+}$ and *Mthfd1l*$^{gt/gt}$ embryos, respectively, compared to the stage before neural tube closure, but there was no significant difference between the apoptotic indices of wild type and nullizygous embryos at either 7–13 or 18–24 somite stages (Figure 8e,f).

3.6 | Deletion of Mthfd1l does not affect neural crest cell specification

The expression patterns of the neural crest cell (NCC) markers *Sox9* and *FoxD3* were determined by whole-mount in situ hybridization. Sox9, a member of the Sox (Sry-type high-mobility-group box) family of transcription factors, regulates neural crest development (Lee & Saint-Jeannet, 2011). *Sox9* is expressed in the prospective neural crest and its expression precedes expression of premigratory neural crest markers (Cheung & Briscoe, 2003). *Sox9* expression was observed in the developing hindbrain, otocyst, cephalic mesenchyme tissue and in some surface ectodermal cells overlying the spinal cord of both *Mthfd1l*$^{+/+}$ and *Mthfd1l*$^{gt/gt}$ embryos (Figure 9a–d). There was no apparent difference in the expression pattern of *Sox9* between *Mthfd1l*$^{+/+}$ and *Mthfd1l*$^{gt/gt}$ embryos. Although *Sox9* was expressed clearly in each somite of the wild type, its expression was not distinctively separated in somites of the nullizygotes. It is not clear if this pattern is due to abnormal somite formation or somite degradation in *Mthfd1l*$^{gt/gt}$ embryos.

The transcription factor *FoxD3* is expressed transiently in neural crest cells prior to delamination (Cheung & Briscoe, 2003) and is involved in the segregation of the neural crest lineage from the neuroepithelium. Whole-mount in situ hybridization revealed expression of *FoxD3* in the dorsal neural tube, otocyst, and some surface ectodermal cells overlying the spinal cord at the 7–13 somite stage (Figure 9e,f). *FoxD3* was extensively expressed in trigeminal ganglion and vestibular-acoustic ganglion, and posterior dorsal neural tube at the 18–24 somite stage (Figure 9g,h). However, there was no apparent difference in the expression of *FoxD3* between genotypes at the 7–13 or 18–24 somite stage. The similarity in expression of *Sox9* and *FoxD3* in *Mthfd1l*$^{+/+}$ and *Mthfd1l*$^{gt/gt}$ embryos suggests that neural crest cell specification is not dramatically affected by loss of MTHFD1L.

4 | CONCLUSIONS

The *Mthfd1l* gene is expressed throughout the mouse embryo at all stages of embryogenesis (Pike et al., 2010; Shin et al., 2014), with higher expression observed in the developing neural folds in embryos prior to neural tube closure. Deletion of *Mthfd1l* delays embryonic development and impairs neural tube closure (Momb et al., 2013) (Table 1). Taken together, these results confirm that *Mthfd1l* is essential for neural tube closure.

Upon sectioning whole embryos through the cranial region, we observed that the head mesenchyme underlying the cranial neural plate was less dense in *Mthfd1l*$^{gt/gt}$ embryos compared to wild-type embryos (Figures 3 and 4). Head mesenchyme is a tissue that surrounds the cranial neural plate. During elevation of the cranial neural folds in mammalian embryos, head mesenchyme undergoes expansion with increases in both cell proliferation and volume of extracellular space, resulting in transformation of the neural plate from biconvex to a “V” shape (Copp, Greene, & Murdoch, 2003). While the expansion is not explained by differential proliferation, it is rather expansion of the extracellular matrix, rich in glycosaminoglycans, that seems to drive the cell translocation (Morris-Wiman & Brinkley, 1990). Cells populating the head mesenchyme contribute to multiple structures such as the smooth and skeletal muscles, skull, cranial nerves, blood vessels and many of the bony elements in the head and face (Zohn, Anderson, & Niswander, 2007).

Proper head mesenchyme formation is believed to be an important factor regulating cranial neural tube closure. In several mouse models lacking genes expressed in the head mesenchyme, such as *Twist* (twist homolog 1), *Cart1* (cartilage homeo protein 1), *Alx3* (aristaless-like homeobox 3), and *Hectd1* (HECT domain containing 1), the embryos develop exencephaly with abnormal head mesenchyme density around the neural folds (Chen & Behringer, 1995; Lakhwani, Garcia-Sanz, & Vallejo, 2010; Zhao, Behringer, & de Crombrugghe, 1996; Zohn et al., 2007). Two of these mouse models support a role for folate-mediated 1C metabolism in head mesenchyme development. NTDs caused by deletion of *Cart1* are preventable by folate supplementation (Zhao et al., 1996), and folic acid was shown to be required for the specific expression of *Alx3* in the head mesenchyme (Lakhwani et al., 2010).

Several cellular processes are essential for proper elevation, apposition, and closure of the cranial neural folds, including neuroepithelial cell proliferation, apoptosis, neural crest cell specification, and head mesenchymal expansion (Honarpour, Gilbert, Lahn, Wang, & Herz, 2001; Lardelli, Williams, Mitsiadis, & Lendahl, 1996; Lufkin, Dierich, LeMeur, Mark, & Chambon, 1991; Weil, Jacobson, & Raff, 1997; Zohn et al., 2007). We sought to understand the effect of *Mthfd1l* deletion on these processes around the time of neural tube closure to better understand the mechanism underlying the sparse mesenchyme phenotype. Using phosphohistone H3 as a marker of cellular mitotic index, we found that *Mthfd1l* deletion decreased cellular proliferation within *Mthfd1l*$^{gt/gt}$ embryonic cranial tissue, but only after neural tube closure had completed (18–24 somite stage) (Figure 6). This result is consistent with other knockout mouse models of 1C metabolism genes that show reduced cellular proliferation during E9.0–E11.5 (after neural tube closure) (Pai et al., 2015; Tang, Santillano, Wlodarczyk, Miranda, & Finnell, 2005). In the current study, we observed no difference in proliferation in 7–13 somite stage embryos (Figure 6). Tuckett and Morriss-Kay reported that proliferation rates do not differ between forebrain, midbrain, and hindbrain regions during early neurulation in rats (4–16 somites) (Tuckett & Morriss-Kay, 1985). It was suggested that the neural epithelium is a fluid structure whose overall shape is strictly controlled, but not by cell number. The reduced cellular proliferation after neural tube closure in *Mthfd1l* mutant embryos may be explained as (a) a primary effect causing failure of cranial neural folds which is incompatible with closure in the hindbrain, although permissive for closure in the forebrain and midbrain; or (b) a secondary effect caused by other dysregulated cellular processes. EdU incorporation in MEFs showed no difference between the two genotypes, suggesting a possible secondary effect (Table 2). Further analyses, such as incorporation of BrdU or radioisotopes, will be required to distinguish between these alternatives.

Apoptosis was investigated using caspase-3, and this assay revealed no difference in the apoptotic process between wild-type and *Mthfd1l*$^{gt/gt}$ embryos in either 7–13 or 18–24 somite stage embryos (Figure 8). We then asked whether *Mthfd1l* deletion impairs neural crest cell specification. However, the expression patterns of neural crest cell markers *Sox9* and *FoxD3* did not differ substantially between wild-type and *Mthfd1l*$^{gt/gt}$ embryos at 7–13 and 18–24 somite stages (Figure 9). These results suggest that defects in cell proliferation or apoptosis prior to neural tube closure are likely not responsible for the aberrant neural tube closure

caused by *Mthfd1l* deletion. Likewise, neural crest cell specification does not appear to be affected by *Mthfd1l* deletion.

It is surprising that *Mthfd1l* deletion did not dramatically impact cellular processes that are known to be important for neural tube closure. Reduced proliferation was observed in null embryos after neural tube closure but not during earlier developmental stages, whereas mesenchyme density was affected in preneurulation embryos (7–13 somite stages). These data suggest a possible mechanistic link between folate-dependent mitochondrially produced formate, mesenchyme formation, and neural tube defects. Supplementation of pregnant dams with formate improved mesenchyme density in *Mthfd1l*$^{gt/gt}$ embryos (Figure 5) and also corrected cell proliferation in the hindbrain neuroepithelium of 18–24 somite *Mthfd1l*$^{gt/gt}$ embryos (compare Figures 6 and 7). Importantly, correction of mesenchyme density in *Mthfd1l*$^{gt/gt}$ embryos by maternal formate supplementation (Figure 5) shows that mitochondrial formate production is critical to support proper mesenchyme formation and neural tube closure. Similar to the *Mthfd1l* mouse model, two additional mouse models are known in which the NTD phenotype is partially rescued by maternal formate supplementation: *Gldc* (glycine decarboxylase) (Pai et al., 2015) and *Slc25a32* (mitochondrial folate transporter) (Kim et al., 2018). In both of these models, mitochondrial folate-mediated 1C metabolism is disrupted, potentially impacting mitochondrial formate production.

How might mitochondrially derived formate play a role in head mesenchyme development? One possibility is its role in supplying 1C units for the synthesis of methyl groups (see Figure 1). Dunlevy et al. reported that disruption of the methylation cycle by inhibitors (ethionine and cycloleucine) or excess methionine causes a reduction in head mesenchyme density (Dunlevy, Burren, Chitty, Copp, & Greene, 2006; Dunlevy, Burren, Mills, et al., 2006). Since greater than 75% of one-carbon units that enter the cytoplasmic methyl cycle are derived from mitochondrially produced formate (Pike et al., 2010), loss of *Mthfd1l* may lead to aberrant methylation. Synthesis of *S*-adenosylmethionine (AdoMet) is critical for chromatin and DNA methylation, which play essential roles during cell differentiation (Bai et al., 2005; Kobayakawa, Miike, Nakao, & Abe, 2007) and cell migration (Horswill, Narayan, Warejcka, Cirillo, & Twining, 2008). Extensive reprogramming of DNA methylation occurs during early embryogenesis (Borgel et al., 2010). Human studies have linked maternal folate status and occurrence of NTDs to tissue-specific DNA hypo- and hypermethylation patterns, with decreased DNA methylation observed in NTD brain tissue compared with normal embryos (Chang et al., 2011). Protein methylation is also active during neural tube development. Rat embryos cultured in methionine-deficient conditions exhibit hypomethylation of neural tube proteins and failure of neural tube closure (Coelho & Klein, 1990). Proper function of the cytoskeleton is required for cranial neural tube closure (Copp et al., 2003), and the cytoskeletal proteins β-actin and tubulin are known to be methylated during neural tube closure (Moephuli, Klein, Baldwin, & Krider, 1997).

It is noteworthy that Mthfd1l is highly expressed in placenta (Prasannan & Appling, 2009; Prasannan, Pike, Peng, Shane, & Appling, 2003). Rosario et al. suggested that maternal folate deficiency causes inhibition of mTOR (mammalian target of rapamycin) signaling, resulting in down-regulation of placental amino acid transporters and subsequent fetal

growth restriction (Rosario, Nathanielsz, Powell, & Jansson, 2017). Therefore, it cannot be ruled out that the effects of formate supplementation could be secondary, ameliorating formate-dependent processes in mothers that support implantation, improve embryonic growth of mutant embryos, or regulate placenta signaling related to embryonic growth, especially on head mesenchyme development. To investigate this effect, transgenic approaches or blastocyst transfers of mutant embryos from a heterozygous mother into a wild-type dam might be used to reduce possible confounding effects of maternal heterozygosity.

Based on the results of the current study, we propose a model to describe the relationship between MTHFD1L expression and neural tube closure in hindbrain development (Figure 10). MTHFD1L, responsible for mitochondrial formate production, is highly expressed in neuroepithelium and underlying paraxial mesoderm. A high density of mesenchymal cells supports elevation of neural plates and formation of dorsolateral hinge points. Inactivation of the *Mthfd1l* gene results in reduced mesenchymal density, leading to inadequate physical forces acting on the neural plates to elevate, ultimately resulting in failure of neural tube closure. Interestingly, expansion of the mesenchyme (specifically paraxial mesoderm) does not accompany neural fold elevation in the spinal region (Copp et al., 2003), and experimental removal of the paraxial mesoderm fails to block spinal neural tube closure (Copp et al., 2003; van Straaten, Hekking, Consten, & Copp, 1993). This model of possible involvement of MTHFD1L in head mesenchyme development is consistent with our observation that MTHFD1L mutation causes exencephaly but not spina bifida.

ACKNOWLEDGMENTS

We thank Dr. Steven A. Vokes for his advice and suggestions and for his critical reading of the manuscript. We also thank Dr. Angel Syrett for her assistance with Figure 10. This work was supported by National Institutes of Health grants F32HD074428 (to J.M.) and HD083809 (to D.R.A).

Funding information

National Institutes of Health, Grant/Award Numbers: HD083809, F32HD074428

REFERENCES

Au KS, Findley TO, & Northrup H. (2017). Finding the genetic mechanisms of folate deficiency and neural tube defects—Leaving no stone unturned. American Journal of Medical Genetics. Part A, 173A, 3042–3057.

Bai S, Ghoshal K, Datta J, Majumder S, Yoon SO, & Jacob ST (2005). DNA methyltransferase 3b regulates nerve growth factor-induced differentiation of PC12 cells by recruiting histone deacetylase 2. Molecular and Cellular Biology, 25, 751–766. [PubMed: 15632075]

Borgel J, Guibert S, Li Y, Chiba H, Schubeler D, Sasaki H, … Weber M. (2010). Targets and dynamics of promoter DNA methylation during early mouse development. Nature Genetics, 42, 1093–1100. [PubMed: 21057502]

Bryant JD, Sweeney SR, Sentandreu E, Shin M, Ipas H, Xhemalce B, … Appling DR (2018). Deletion of the neural tube defect–associated gene Mthfd1l disrupts one-carbon and central energy metabolism in mouse embryos. Journal of Biological Chemistry, 293, 5821–5833. [PubMed: 29483189]

Chang H, Zhang T, Zhang Z, Bao R, Fu C, Wang Z, … Wu J. (2011). Tissue-specific distribution of aberrant DNA methylation associated with maternal low-folate status in human neural tube defects. The Journal of Nutritional Biochemistry, 22, 1172–1177. [PubMed: 21333513]

Chen ZF, & Behringer RR (1995). twist is required in head mesenchyme for cranial neural tube morphogenesis. Genes and Development, 9, 686–699. [PubMed: 7729687]

Cheung M, & Briscoe J. (2003). Neural crest development is regulated by the transcription factor Sox9. Development, 130, 5681–5693. [PubMed: 14522876]

Coelho CN, & Klein NW (1990). Methionine and neural tube closure in cultured rat embryos: Morphological and biochemical analyses. Teratology, 42, 437–451. [PubMed: 2256006]

Copp AJ, Greene ND, & Murdoch JN (2003). The genetic basis of mammalian neurulation. Nature Reviews. Genetics, 4, 784–793.

Dunlevy LP, Burren KA, Chitty LS, Copp AJ, & Greene ND (2006). Excess methionine suppresses the methylation cycle and inhibits neural tube closure in mouse embryos. FEBS Letters, 580, 2803–2807. [PubMed: 16674949]

Dunlevy LP, Burren KA, Mills K, Chitty LS, Copp AJ, & Greene ND (2006). Integrity of the methylation cycle is essential for mammalian neural tube closure. Birth Defects Research. Part A, Clinical and Molecular Teratology, 76, 544–552. [PubMed: 16933307]

Hibbard ED, & Smithells RW (1965). Folic acid metabolism and human embryopathy. Lancet, 1(7398), 1254.

Hobbs CA, Shaw GM, Werler MM, & Mosley B. (2010). Folate status and birth defect risk. Epidemiological perspective In Bailey LB (Ed.), Folate in health and disease (2nd ed, 133–153). Boca Raton, FL: CRC Press, Taylor & Francis Group.

Honarpour N, Gilbert SL, Lahn BT, Wang X, & Herz J. (2001). Apaf-1 deficiency and neural tube closure defects are found in fog mice. Proceedings of the National Academy of Sciences of the United States of America, 98, 9683–9687. [PubMed: 11504943]

Horswill MA, Narayan M, Warejcka DJ, Cirillo LA, & Twining SS (2008). Epigenetic silencing of maspin expression occurs early in the conversion of keratocytes to fibroblasts. Experimental Eye Research, 86, 586–600. [PubMed: 18291368]

Juriloff DM, & Harris MJ (2018). Insights into the etiology of mammalian neural tube closure defects from developmental, genetic and evolutionary studies. Journal of Developmental Biology, 6, 40.

Kim J, Lei Y, Guo J, Kim SE, Wlodarczyk BJ, Cabrera RM, … Finnell RH (2018). Formate rescues neural tube defects caused by mutations in Slc25a32. Proceedings of the National Academy of Sciences of the United States of America, 115, 4690–4695. [PubMed: 29666258]

Kobayakawa S, Miike K, Nakao M, & Abe K. (2007). Dynamic changes in the epigenomic state and nuclear organization of differentiating mouse embryonic stem cells. Genes to Cells, 12, 447–460. [PubMed: 17397393]

Lakhwani S, Garcia-Sanz P, & Vallejo M. (2010). Alx3-deficient mice exhibit folic acid-resistant craniofacial midline and neural tube closure defects. Developmental Biology, 344, 869–880. [PubMed: 20534379]

Lardelli M, Williams R, Mitsiadis T, & Lendahl U. (1996). Expression of the Notch 3 intracellular domain in mouse central nervous system progenitor cells is lethal and leads to disturbed neural tube development. Mechanisms of Development, 59, 177–190. [PubMed: 8951795]

Lee YH, & Saint-Jeannet JP (2011). Sox9 function in craniofacial development and disease. Genesis, 49, 200–208. [PubMed: 21309066]

Lufkin T, Dierich A, LeMeur M, Mark M, & Chambon P. (1991). Disruption of the Hox-1.6 homeobox gene results in defects in a region corresponding to its rostral domain of expression. Cell, 66, 1105–1119. [PubMed: 1680563]

Moephuli SR, Klein NW, Baldwin MT, & Krider HM (1997). Effects of methionine on the cytoplasmic distribution of actin and tubulin during neural tube closure in rat embryos. Proceedings of the National Academy of Sciences of the United States of America, 94, 543–548. [PubMed: 9012820]

Momb J, Lewandowski JP, Bryant JD, Fitch R, Surman DR, Vokes SA, & Appling DR (2013). Deletion of Mthfd1l causes embryonic lethality and neural tube and craniofacial defects in mice. Proceedings of the National Academy of Sciences of the United States of America, 110, 549–554. 10.1073/pnas.1211199110 [PubMed: 23267094]

Morris-Wiman J, & Brinkley LL (1990). The role of the mesenchyme in mouse neural fold elevation. I. Patterns of mesenchymal cell distribution and proliferation in embryos developing in vitro. American Journal of Anatomy, 188(2), 121–132. 10.1002/aja.1001880203 [PubMed: 2375278]

Nikolopoulou E, Galea GL, Rolo A, Greene ND, & Copp AJ (2017). Neural tube closure: Cellular, molecular and biomechanical mechanisms. Development, 144, 552–566. [PubMed: 28196803]

Pai YJ, Leung K-Y, Savery D, Hutchin T, Prunty H, Heales S, … Greene NDE (2015). Glycine decarboxylase deficiency causes neural tube defects and features of non-ketotic hyperglycinemia in mice. Nature Communications, 6, 6388.

Pike ST, Rajendra R, Artzt K, & Appling DR (2010). Mitochondrial C1-THF synthase (MTHFD1L) supports flow of mitochondrial one-carbon units into the methyl cycle in embryos. Journal of Biological Chemistry, 285, 4612–4620. [PubMed: 19948730]

Prasannan P, & Appling DR (2009). Human mitochondrial C1-tetrahydrofolate synthase: Submitochondrial localization of the full-length enzyme and characterization of a short isoform. Archives of Biochemistry and Biophysics, 481, 86–93. [PubMed: 18996079]

Prasannan P, Pike S, Peng K, Shane B, & Appling DR (2003). Human mitochondrial C1-tetrahydrofolate synthase: Gene structure, tissue distribution of the mRNA, and immunolocalization in Chinese hamster ovary cells. Journal of Biological Chemistry, 278, 43178–43187. [PubMed: 12937168]

Rosario FJ, Nathanielsz PW, Powell TL, & Jansson T. (2017). Maternal folate deficiency causes inhibition of mTOR signaling, down-regulation of placental amino acid transporters and fetal growth restriction in mice. Scientific Reports, 7, 3982. [PubMed: 28638048]

Shin M, Bryant JD, Momb J, & Appling DR (2014). Mitochondrial MTHFD2L is a dual redox cofactor-specific methylenetetrahydrofolate dehydrogenase/methenyltetrahydrofolate cyclohydrolase expressed in both adult and embryonic tissues. Journal of Biological Chemistry, 289, 15507–15517. [PubMed: 24733394]

Tang LS, Santillano DR, Wlodarczyk BJ, Miranda RC, & Finnell RH (2005). Role of Folbp1 in the regional regulation of apoptosis and cell proliferation in the developing neural tube and craniofacies. American Journal of Medical Genetics. Part C, Seminars in Medical Genetics, 135C, 48–58.

Theiler K. (1989). The house mouse: Atlas of embryonic development. New York, NY: Springer-Verlag.

Tibbetts AS, & Appling DR (2010). Compartmentalization of mammalian folate-mediated one-carbon metabolism. Annual Review of Nutrition, 30, 57–81.

Tuckett F, & Morriss-Kay GM (1985). The kinetic behaviour of the cranial neural epithelium during neurulation in the rat. Journal of Embryology and Experimental Morphology, 85, 111–119. [PubMed: 3989446]

van Straaten HW, Hekking JW, Consten C, & Copp AJ (1993). Intrinsic and extrinsic factors in the mechanism of neurulation: Effect of curvature of the body axis on closure of the posterior neuropore. Development, 117, 1163–1172. [PubMed: 8325240]

Weil M, Jacobson MD, & Raff MC (1997). Is programmed cell death required for neural tube closure? Current Biology, 7, 281–284. [PubMed: 9094312]

Wilkinson DG (Ed.). (1998). In situ hybridization: A practical approach (2nd ed). Oxford, NY: Oxford University Press.

Yamaguchi Y, & Miura M. (2013). How to form and close the brain: Insight into the mechanism of cranial neural tube closure in mammals. Cellular and Molecular Life Sciences, 70(17), 3171–3186. 10.1007/s00018-012-1227-7 [PubMed: 23242429]

Zhao Q, Behringer RR, & de Crombrugghe B. (1996). Prenatal folic acid treatment suppresses acrania and meroanencephaly in mice mutant for the Cart1 homeobox gene. Nature Genetics, 13, 275–283. [PubMed: 8673125]

Zohn IE, Anderson KV, & Niswander L. (2007). The Hectd1 ubiquitin ligase is required for development of the head mesenchyme and neural tube closure. Developmental Biology, 306, 208–221. [PubMed: 17442300]

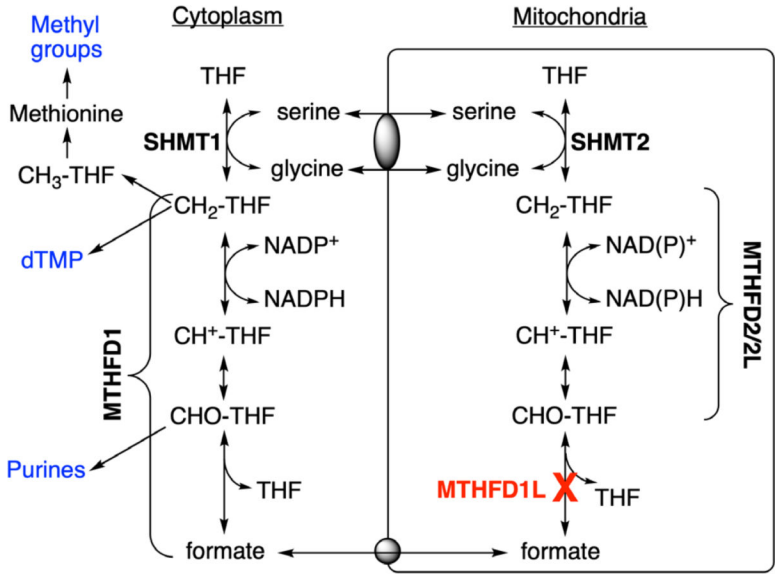

FIGURE 1.

Compartmentalization of folate-dependent one-carbon metabolism. In mammalian mitochondria, monofunctional MTHFD1L catalyzes the 10-formyl-THF (CHO-THF) synthetase reaction. This enzyme is missing in *Mthfd1l* knockout mice. Bifunctional MTHFD2 or MTHFD2L enzymes catalyse 5,10-methenyl-THF (CH^+-THF) cyclohydrolase and 5,10-methylene-THF (CH_2-THF) dehydrogenase activities. MTHFD1 is the cytoplasmic trifunctional C_1-THF synthase that catalyzes 10-formyl-THF synthetase, 5,10-methenyl-THF cyclohydrolase, and 5,10-methylene-THF dehydrogenase activities. SHMT1 and SHMT2 represent cytoplasmic and mitochondrial serine hydroxymethyltransferase isozymes, respectively. Gray ovals represent putative metabolite transporters. CH_3-THF, 5-methyl-THF; dTMP, thymidylate

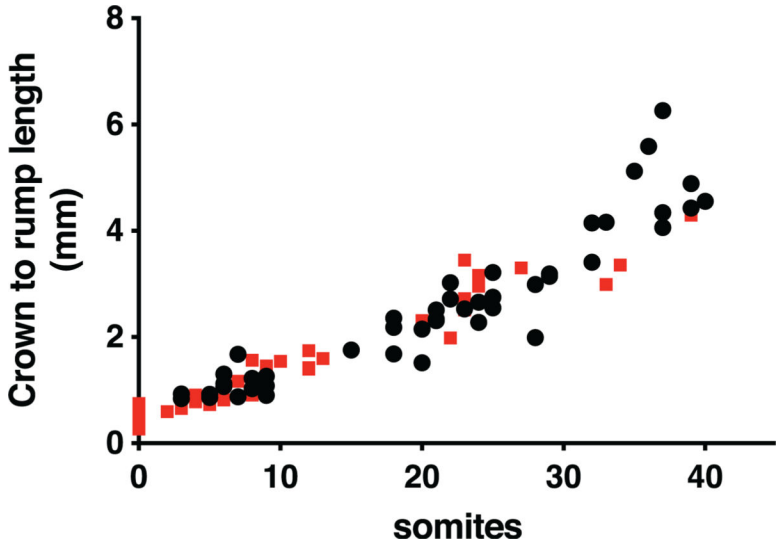

FIGURE 2.

Plots of crown-to-rump length versus somite number for individual embryos do not show difference between genotypes. ■, wild-type embryos; ●, nullizygous embryos. The lines are not significantly different for somite numbers ≤35 ($p = .13$). If somite numbers >35 are included, $p = .013$

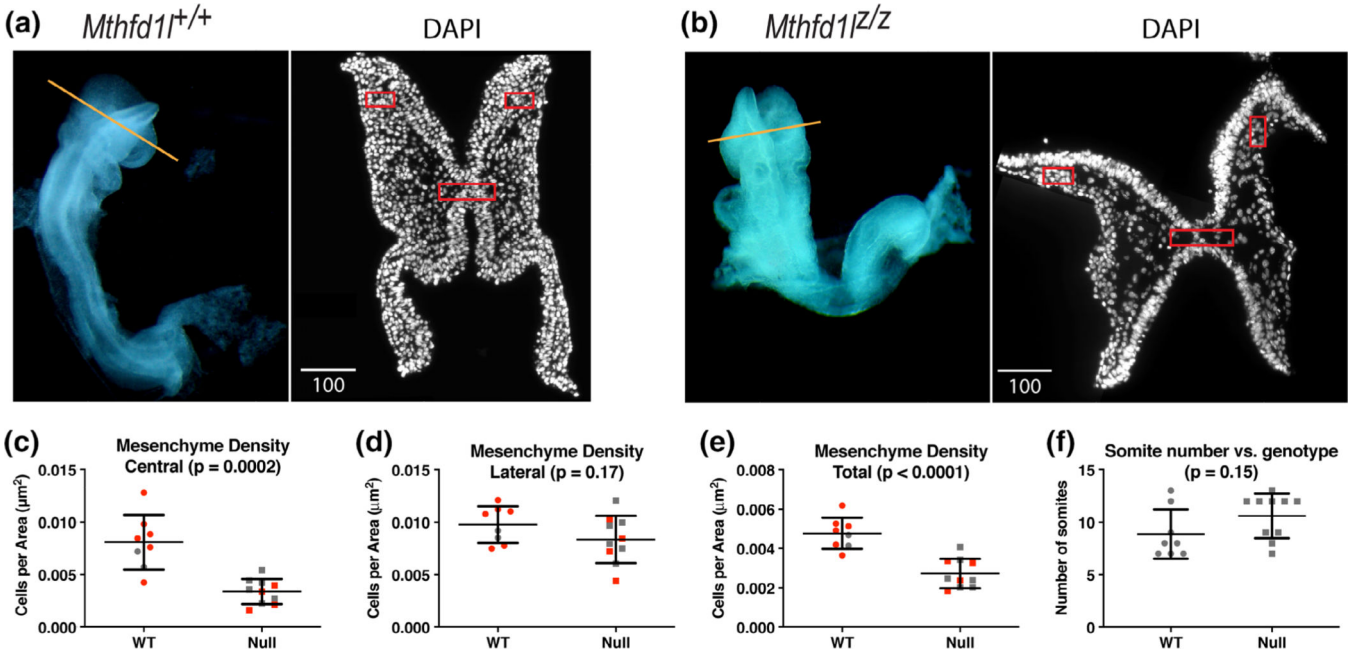

FIGURE 3.

Deletion of *Mthfd1l* causes reduced head mesenchyme density at 7–13 somite stages. Representative transverse cryosections of the cranial region of *Mthfd1l*$^{+/+}$ (wild type) (a) and *Mthfd1l*$^{z/z}$ (nullizygous) (b) embryos stained with DAPI. Straight line in the whole embryos indicates the level of sections. Scale bars indicate microns. (c–e) Head mesenchyme density is quantified for central and lateral areas (boxed regions in sections), as well as the total mesenchyme. Red symbols indicate sections from 7 to 9 somite stage embryos; gray symbols indicate sections from 10 to 13 somite stage embryos. Total mesenchyme density was significantly lower in nullizygous embryos from both the 7–9 (p = .0036) and 10–13 somite stage subgroups (p = .0382). Central mesenchyme density was significantly lower in nullizygous embryos from both the 7–9 (p = .0044) and 10–13 somite stage subgroups (p = .0282). (f) Somite number versus genotype of embryos in this study. n = eight embryos in wild-type and nine embryos in nullizygotes with two to three sections analyzed per embryo. p values were calculated by Mann–Whitney U test

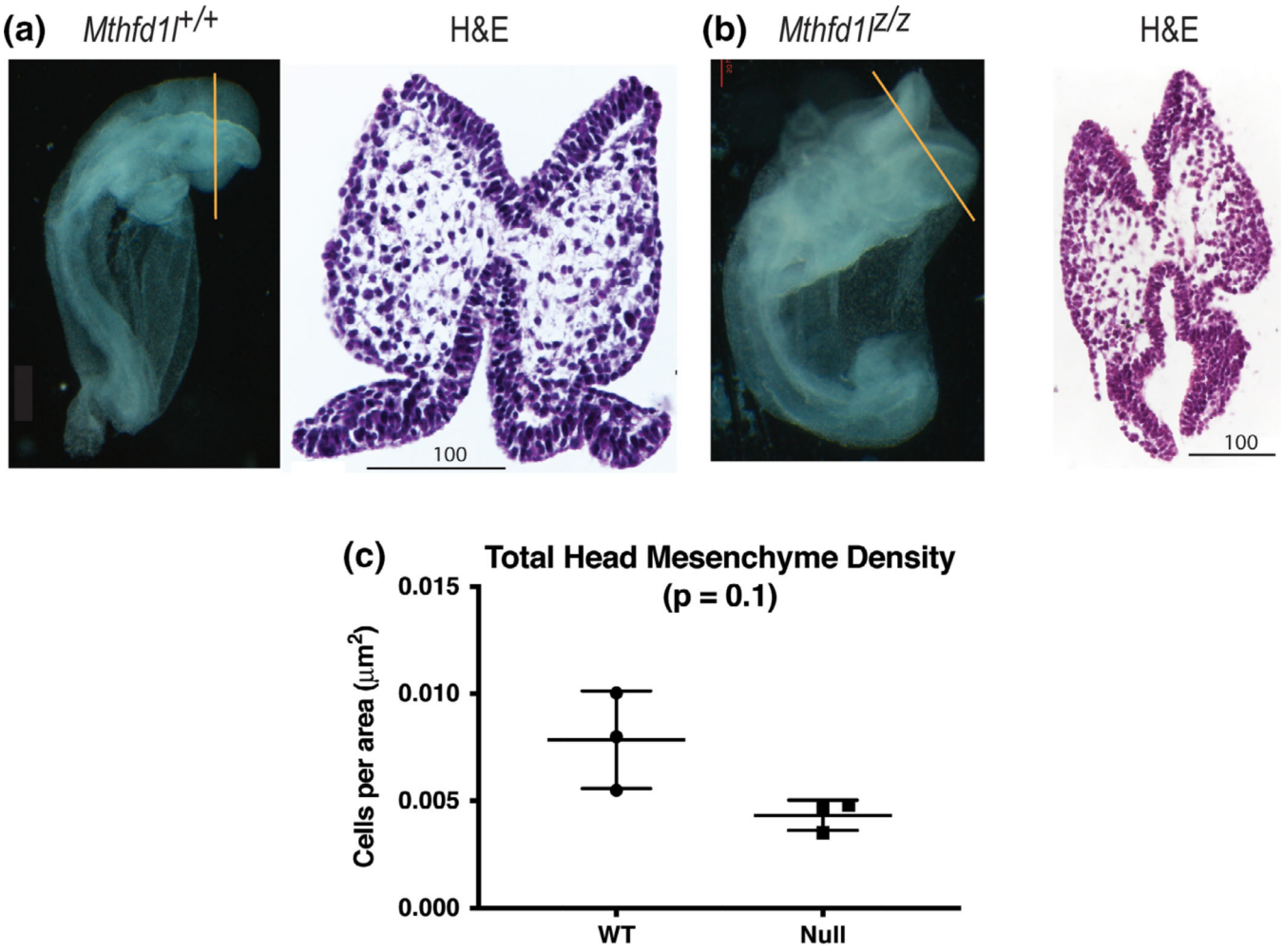

FIGURE 4.

Head mesenchyme density in paraffin sections in 7–13 somite stage embryos. Representative transverse paraffin-embedded sections of *Mthfd1l*$^{+/+}$ (wild-type) (a) and *Mthfd1l*$^{z/z}$ (nullizygous) (b) embryos were stained with hematoxylin and eosin (H&E). Straight line in the whole embryos indicates the level of sections. Scale bars indicate microns. (c) Total head mesenchyme density. *n* = three embryos in each genotype with values from three sections averaged per embryo. *p* value was calculated by Mann–Whitney U test

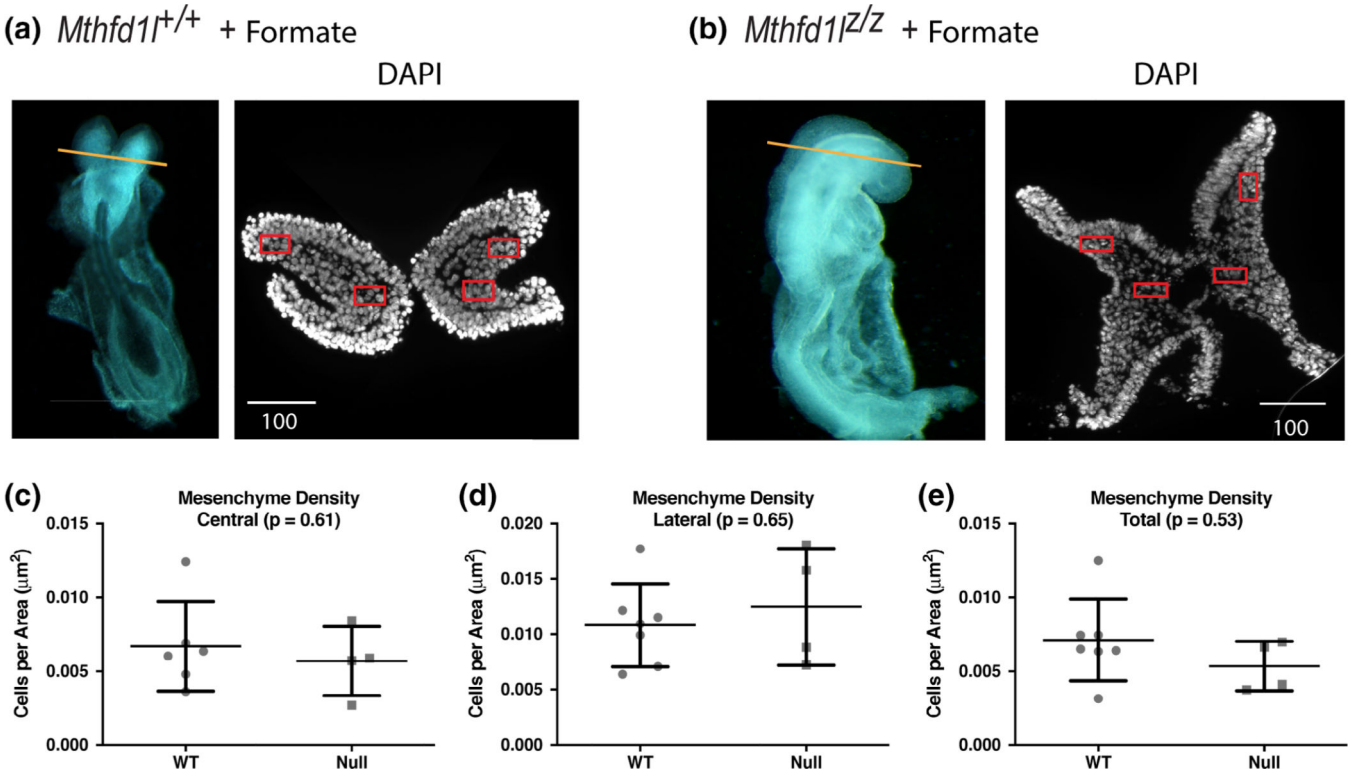

FIGURE 5.

Maternal formate supplementation improves head mesenchyme density in *Mthfd1l* mutant embryos at 7–13 somite stages. (a, b) Representative transverse cryosections of the cranial region of *Mthfd1l*$^{+/+}$ (wild-type) and *Mthfd1l*$^{z/z}$ (nullizygous) embryos were stained with DAPI for nuclei. Straight line in the whole embryos indicates the level of sections. Scale bars indicate microns. (c–e) Head mesenchyme density is quantified for central and lateral areas (boxed regions in DAPI stained sections), as well as the total mesenchyme. n = six embryos in formate-supplemented wild type and four embryos in formate-supplemented nullizygotes with values from two to four sections averaged per embryo. p values were calculated by Mann–Whitney U test

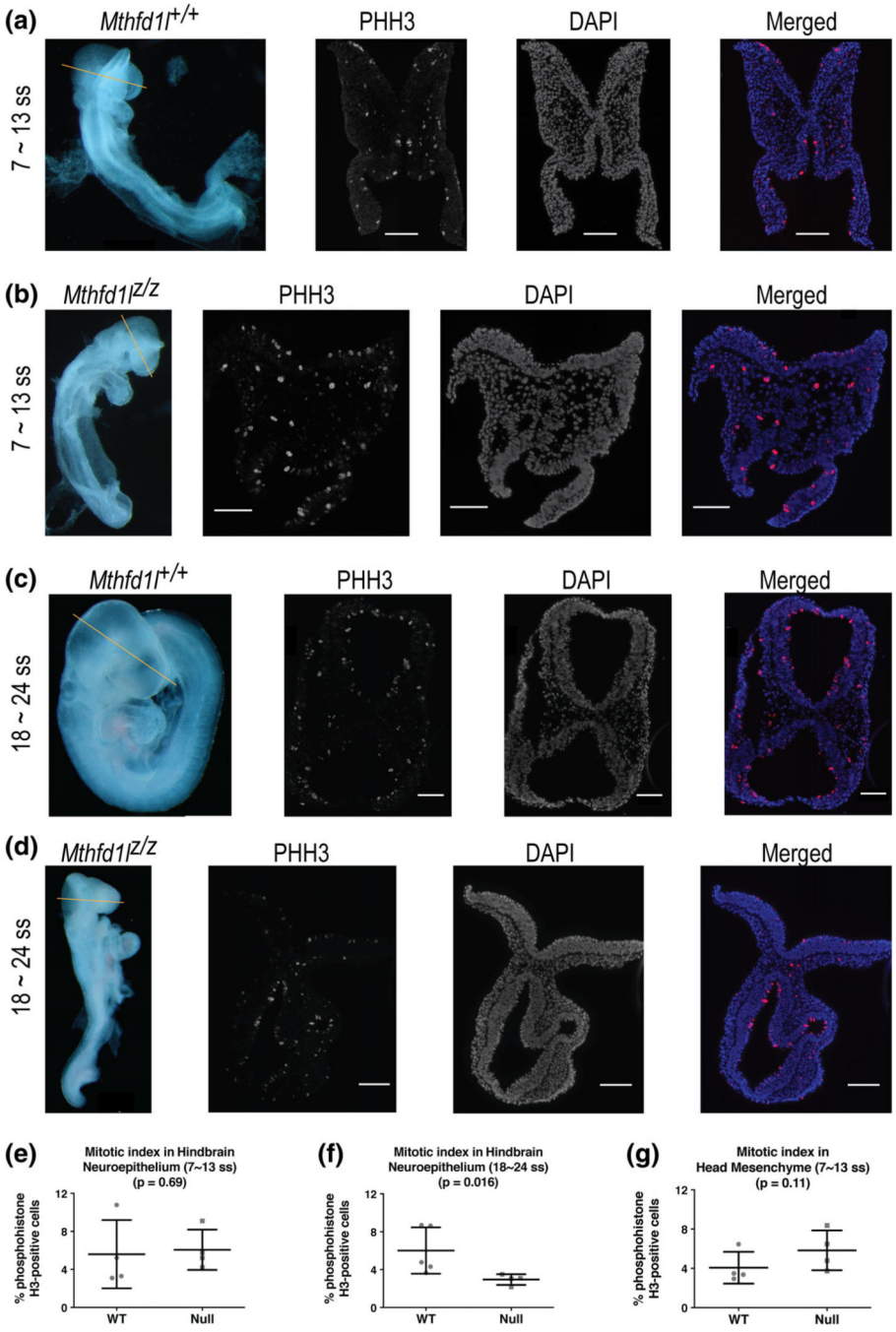

FIGURE 6.

Deletion of *Mthfd1l* causes reduced proliferation in neuroepithelium at 18–24 somite stages, at the time of completion of neural tube closure. Straight line in whole embryos indicates the level of sections. Sections were stained for phosphohistone H3 (PHH3) and DAPI for nuclei. In the merged images, PHH3 staining is red and DAPI staining is blue. (a, c) Representative sections from *Mthfd1l*$^{+/+}$ (wild-type) embryo at 7–13 (a) or 18–24 somite stages (c). (b, d) Representative sections from *Mthfd1l*$^{z/z}$ (nullizygous) embryo at 7–13 (b) or 18–24 somite stages (d). Scale bars indicate 100 microns. (e, f) The mitotic index (% phosphohistone H3-

positive cells) in neuroepithelium was quantified at the developing hindbrain. (g) The mitotic index was quantified in head mesenchyme at 7–13 somite stages. In (e–g), n = four embryos in each genotype with values from three to four sections averaged per embryo. Error bars represent standard deviation and p value was calculated by Mann–Whitney U test

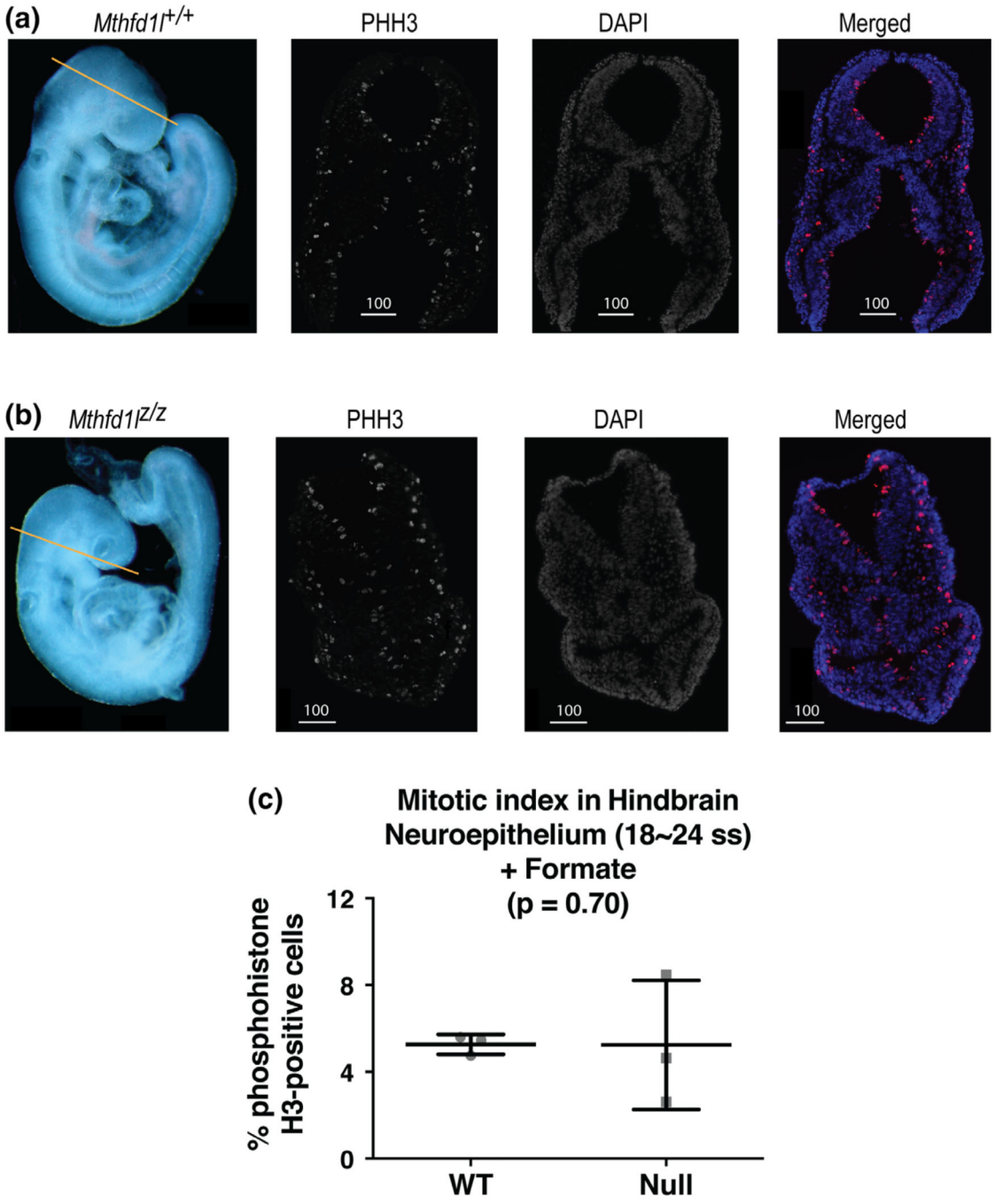

FIGURE 7.

Maternal formate supplementation improves reduced proliferation in neuroepithelium of *Mthfd1l* mutant embryos at 18–24 somite stages, at the time of completion of neural tube closure. Straight line in whole embryos (a, b) indicates the level of sections. Sections were stained for phosphohistone H3 (PHH3) and DAPI for nuclei. In the merged images, PHH3 staining is red and DAPI staining is blue. (a) Representative sections from *Mthfd1l*$^{+/+}$ (wild-type) embryo. (b) Representative sections from *Mthfd1l*$^{z/z}$ (nullizygous) embryo. Scale bars indicate microns. (c) The mitotic index (% phosphohistone H3-positive cells) in

neuroepithelium was quantified at the developing hindbrain. n = three embryos for both genotypes and the plot represents mean value of three to four sections per embryo. Error bars represent standard deviation, and p value was calculated by Mann–Whitney U test

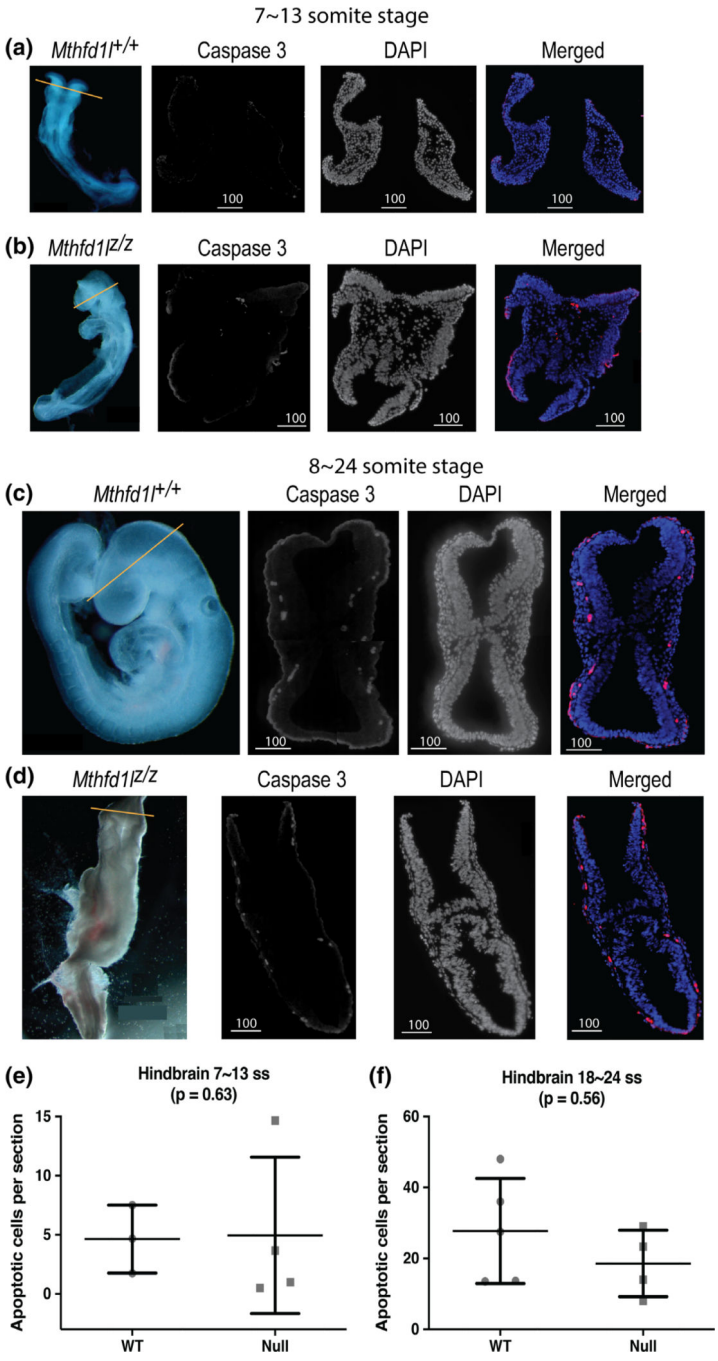

FIGURE 8.

Deletion of *Mthfd1l* does not affect apoptosis during early cranial neural tube closure (7–13 somite stages), nor at the time of completion of neural tube closure (18–24 somite stages). Straight line in whole embryos indicates the level of sections. Sections were stained for caspase 3 and DAPI for nuclei. In the merged images, caspase 3 staining is red and DAPI staining is blue. Contrast was increased here to enhance image clarity for publication. (a, b) Representative sections from *Mthfd1l*$^{+/+}$ (wild-type) and *Mthfd1l*$^{z/z}$ (nullizygous) embryos at 7–13 somite stages. (c, d) Representative sections from Mthfd1l$^{+/+}$ (wild-type) and

Mthfd1l$^{z/z}$ (nullizygous) embryos at 18–24 somite stages. (e, f) The apoptotic index (number of cleaved caspase 3-positive cells per section) was determined at the level of developing hindbrain (to the level of first branchial arch). *n* = three wild-type and four nullizygous embryos (e); *n* = five wild-type and four nullizygous embryos (f). Three to four sections were averaged per embryo. *p* value was calculated by Mann–Whitney U test

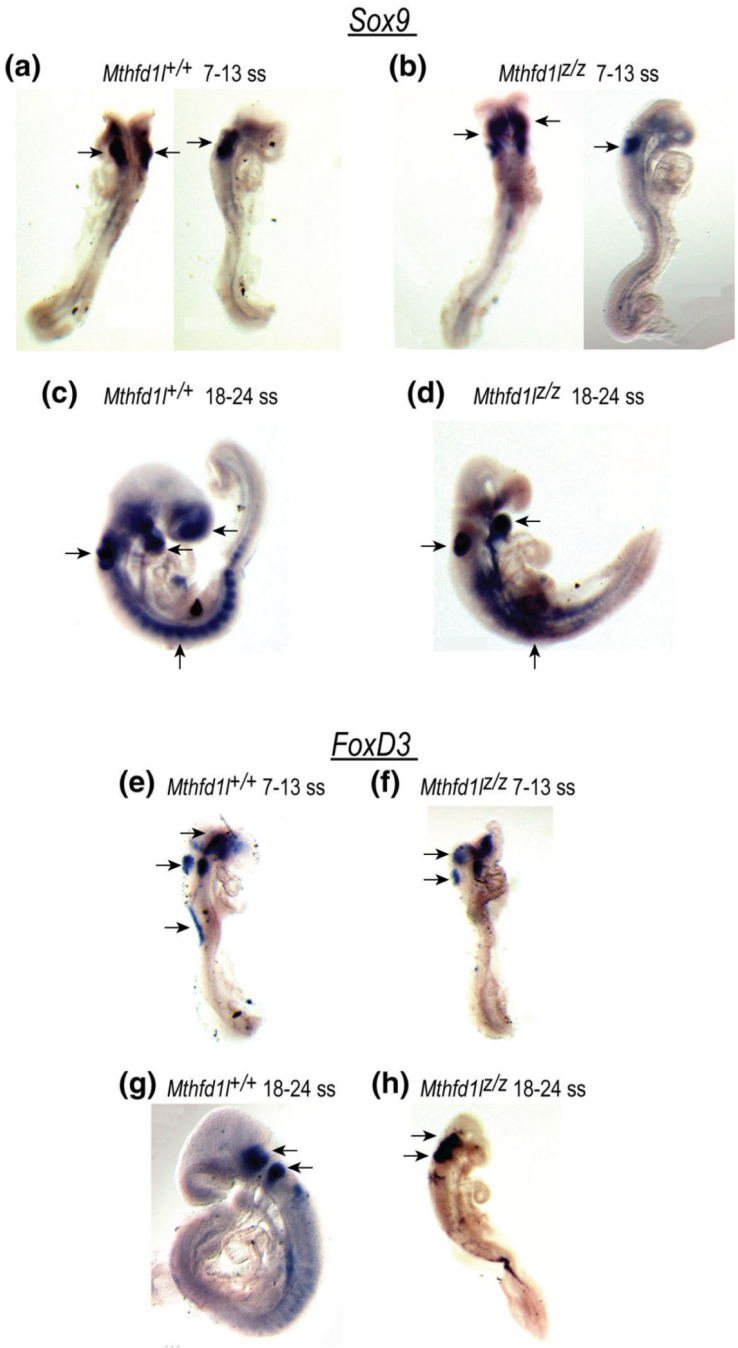

FIGURE 9.

Deletion of *Mthfd1l* does not affect neural crest cell specification during neural tube closure. *Sox9* and *FoxD3* expression were visualized by whole mount in situ hybridization. (a–d) *Sox9* expression in premigratory and migrating neural crest cells in the developing forebrain, hindbrain, otocyst, head mesenchyme, somites, and the branchial arches. (e–h) *FoxD3* expression in premigratory neural crest cells in the dorsal neural tube, otocyst, surface ectodermal cells overlying the spinal cord, trigeminal ganglion and vestibular-acoustic ganglion (arrows)

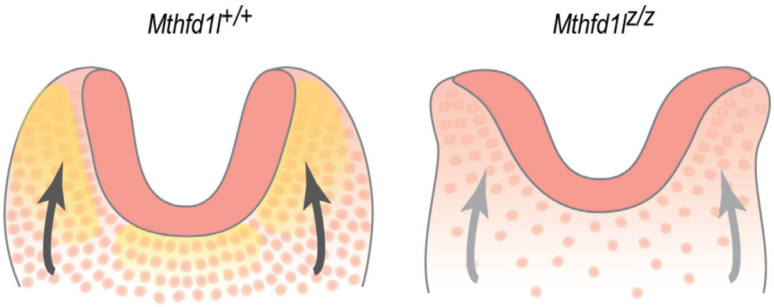

FIGURE 10.

Schematic illustration of the cranial mesenchyme during neural fold elevation. (a) Normal elevation of neural plates is supported by head mesenchymal cells in wild type embryos. (b) Apposition and fusion of neural plates are failed in *Mthfd1l* nullizygotes. Neuroepithelium and mesenchyme are shown in dark and light pink, respectively. Yellow shading in panel (a) indicates MTHFD1L expression. Arrows indicate physical forces generated by mesenchyme acting on the neural plates that drive neural fold elevation

TABLE 1

Mthfd1l nullizygous mice have delayed embryonic growth and open neural tube in the cranial region

Age	Embryo genotype	No. of embryos	No. of somites (mean ± *SD*)	Crown to rump length (mm) (mean ± *SD*)	Neural tube open (no. of embryos)	Conforms to Mendelian ratio?
E8.5/E8.75	*Mthfd1l*$^{+/+}$	39	7.0 ± 3.4	1.15 ± 0.25	100% (39)	Yes
	Mthfd1l$^{z/+}$	71	5.7 ± 3.6	1.08 ± 0.24	100% (71)	$p = .11$
	Mthfd1l$^{z/z}$	23	1.6 ± 2.3*	0.68 ± 0.18*	100% (23)	
E9.5	*Mthfd1l*$^{+/+}$	49	21.9 ± 3.1	2.39 ± 0.50	0% (0)	Yes
	Mthfd1l$^{z/+}$	74	21.8 ± 3.2	2.37 ± 0.46	4% (3)	$p = .07$
	Mthfd1l$^{z/z}$	29	10.5 ± 3.6*	1.46 ± 0.32*	97% (28)	
E10.5	*Mthfd1l*$^{+/+}$	45	33.5 ± 5.7	4.07 ± 1.18	2% (1)	No
	Mthfd1l$^{z/+}$	79	32.6 ± 5.3	4.13 ± 0.84	9% (7)	$p = .02$
	Mthfd1l$^{z/z}$	22	23.9 ± 5.1*	2.75 ± 0.67*	68% (15)[a]	

Note: Embryos were dissected from a total of 78 dams at each indicated age. Numbers of somites in *Mthfd1l*$^{z/z}$ were statistically lower compared to *Mthfd1l*$^{+/+}$ ($p < .0001$ by one-way ANOVA for each age group; asterisk indicates significant difference in *Mthfd1l*$^{z/z}$ compared with *Mthfd1l*$^{+/+}$ or *Mthfd1l*$^{z/+}$at the $p < .05$ level by Bonferroni's multiple comparison test). Number of embryos showing partially or completely open neural tube in the head were counted. Mendelian observed and expected ratios were compared the using Chi-square test.

[a]Mutant embryos whose neural tubes had closed were small, pale, and/or having a wavy neural tube and abnormally formed heads.

TABLE 2

Deletion of *Mthfd1l* does not affect proliferation in MEFs

	% EdU			% PHH3		
Media/genotype	**WT**	**Null**	***p***	**WT**	**Null**	***p***
DMEM	19.2 ± 2.7	25.4 ± 3.5	.13	16.3 ± 6.9	19.3 ± 5.1	.48
MEM	27.8 ± 2.0	32.1 ± 4.8	.48	17.4 ± 6.6	16.7 ± 5.6	.94
MEM+F	24.5 ± 1.9	26.6 ± 2.0	.31	15.1 ± 5.7	15.8 ± 4.4	.59

Note: In cultured embryonic fibroblasts, cell cycle analysis was performed using ethynyl-deoxyuridine (EdU) incorporation for labeling cells in S-phase and phosphohistone H3 (PHH3) staining for labeling cells in mitosis. The experiment was conducted in different culture media condition: DMEM, nutrient-rich medium; MEM, nutrient-limited medium; MEM+F, nutrient-limited medium with formate supplementation. *p* value was calculated by Mann–Whitney U test.

TABLE 3

Maternal formate supplementation improves delayed embryonic growth and partially prevents defective neural tube closure in *Mthfd1l* nullizygous embryos

Age	Genotype	Embryos	Somites (mean ± *SD*)	Crown to rump length (mm) (mean ± *SD*)	Neural tube open (embryos)	Conforms to Mendelian ratio?
E8.75	*Mthfd1l*$^{+/+}$	10	7.4 ± 2.3	0.97 ± 0.30	100% (10)	Yes
	Mthfd1l$^{gt/+}$	20	7.2 ± 3.3	1.11 ± 0.23	100% (20)	$p = .85$
	Mthfd1l$^{gt/gt}$	9	4.6 ± 3.8	0.84 ± 0.42	100% (8)	
E9.5	*Mthfd1l*$^{+/+}$	16	22.3 ± 2.8	2.44 ± 0.52	6% (1)	Yes
	Mthfd1l$^{gt/+}$	27	21.7 ± 3.4	2.44 ± 0.56	11% (3)	$p = .86$
	Mthfd1l$^{gt/gt}$	14	17.6 ± 3.2*	1.83 ± 0.40*	79% (11)	

Note: Embryos were dissected from a total of 15 formate-supplemented dams. Numbers of somites in *Mthfd1l*$^{gt/gt}$ were statistically lower compared to *Mthfd1l*$^{+/+}$ only at E9.5 ($p < .001$ by one-way ANOVA; asterisk indicates significant difference in *Mthfd1l*$^{gt/gt}$ compared with *Mthfd1l*$^{+/+}$ at the $p < .001$ level by Bonferroni's multiple comparison test). Number of embryos showing partially or completely open neural tube in the head were counted. Mendelian observed and expected ratios were compared the using Chi-square test.